Investigating the Applicability of Discontinuous Galerkin Methods Towards Structural Health Monitoring in Transportation

Salah-Eddine Hebaz, Farouk Benmeddour, Emmanuel Moulin, Jamal Assaad

Investigating the Applicability of Discontinuous Galerkin Methods Towards Structural Health Monitoring in Transportation

Salah-Eddine Hebaz *, Farouk Benmeddour **, Emmanuel Moulin, Jamal Assad
IEMN, Opto-Acousto-Electronics Departement, UMR CNRS 8520
University of Valenciennes and Hainaut-Cambrésis, 59313 Valenciennes cedex 9 - France.
Email address * : Salah-Eddine.Hebaz@univ-valenciennes.fr
Email address ** : Farouk.Benmeddour@univ-valenciennes.fr

Abstract*—Ultrasonic guided waves offer an efficient means of rapid non-destructive inspection over long distances. Several researches has been conducted to study and modelise efficiently the propagation of these waves in large structures with arbitrary cross-sections like rails, bars, tubes, and plates. Classical numerical methods such as the finite element method (FEM), the semi-analytical finite element method (SAFE), the hybrid method FEM-SAFE, etc. have proved successful in this regard, but still have a major drawback: the high consumption of resources (memory and CPU time). Recently, the discontinuous Galerkin finite element method (DG-FEM) has revolutionised computations in the time domain through its potential in terms of applications and facilities it provides. In this work, the potential benefits of a class of discontinuous methods namely the interior penalty discontinuous Galerkin methods (IPDG) in the frequency domain are investigated by performing a modal analysis of a finite structure. The natural frequencies and vibration modes are searched via the eigenvalue problem derived from the discretisation of the Helmholtz problem with free boundaries, in one dimension of space. In line with the work of literature, it was found that the resulting solutions are correct and free of spurious modes. In addition, the discontinuous formulation provides an interesting algebraic system with a block tridiagonal stiffness matrix and a diagonal block mass matrix. Therefore, the eigenproblem can be reduced from a generalised problem to a standard one. For large size problems, this can lead to a significant gain in computation time. Moreover, it retains its block-tridiagonal form for which effective and well suited for parallel implementation block algorithms are developed. Thus, the DG-FEM allows a double gain strategy in computation time/memory consumption and achieving high order accuracy.

Keywords*—Structural health monitoring (SHM), Interior penalty discontinuous Galerkin methods (IPDG), Eigenvalue problem.

I. Introduction

The use of analysis tools such as numerical models is a major asset in structural health monitoring (SHM) field, particularly for non-destructive evaluation (NDE) systems using ultrasonic guided waves since it deals with more complex wave propagation phenomenon [1].

In the last decade, many researches has been conducted to study and modelise the propagation of these waves in arbitrary cross-section waveguides (rod, plate, tube, etc.). Several numerical techniques have been developed to overcome the limitations of analytical approaches exclusive to simple geometries [2] [3]. First, the semi-analytical finite element method (SAFE) has been demonstrated very practical for dispersion curves calculations and vibration modes [4] [5]. It allows to model the propagation in an arbitrary cross-section waveguide only from its section. Consequently, any complex section can be treated and the calculation time is constant regardless of the length of the relevant guide. Then, the hybrid method FEM-SAFE allowed to study, predict and facilitate interpretation of the wave interaction with different types of defects. It consists of modeling the damage in the waveguide locally, considering only the faulty portion. Thus, structures with complex defects can be treated effectively and in 2 and in 3 dimensions (for more details see [6]).

However, despite their success and economical scheme, modeling real railway transport structures remained tedious. As the size of the damage is reduced, it is necessary to go up in frequency. Therefore, the mesh should be much finer resulting in an increased resource consumption (CPU time and memory demand) and/or a great error causing an inaccurate numerical solution. Accordingly, modeling beyond certain frequency ranges is a major challenge to date [7]; performing a parametric study of different types of damages remains very difficult.

Recently, discontinuous Galerkin finite element methods (DG-FEM) has revolutionised the calculations in the time domain due to their potential in terms of applications and facilities they provide: geometric flexibility, high order local approximations, naturally parallelisable, etc. Due to the local nature of a discontinuous formulation, the solution is sought at the elementary level to build afterwards the global solution; no need to assemble global matrices, which greatly reduces the memory demand. Moreover, the possibility of parallel computing allows a considerable time gain. It uses the same space of interpolating functions as the standard method but with a relaxed or weak continuity in the inter-elements boundaries. It was first introduced by Reed and Hill in [8] to solve the neutron transport equation. Its recent history and developments were re-examined in [9] [10] [11].

Yet, since their introduction, these DG methods were the prerogative of time domain and boundary value problems. The development of such methods in the frequency

domain, precisely for eigenvalue problems (EP) stayed very limited in the literature; This can be justified by the appearance of fictional or parasite modes, i.e. solutions that have no physical meaning. Later on, the issue of usability of discontinuous methods for spectral approximation (i.e. computation of eigenvalues and normal modes) was addressed for the Maxwell and the Laplace eigenvalue problems in 2 dimensions respectively in the work of Hesthaven et al. [12] and of Antonietti et al. [13]. It was found that actually several variants of DG methods provide a spectrally correct solution and free of spurious modes. An overview can be found in [14], Chapter 8.

In this paper, we examine the potential benefits of a class of discontinuous methods namely the interior penalty family (IPDG) for a subsequent application in the field of SHM by ultrasonic guided waves. The aim of this work is to perform a modal analysis of a finite structure in free regime, through which the properties of the method and the resulting eigenvalue problem can be investigated.

In this sense, a simple waveguide that is a long straight bar with free ends with a uniform cross section along the direction of propagation is considered. Its behavior analysis consist of finding the wave numbers and the corresponding normal modes through the resulting eigenvalue problem. We restrict this study to the one dimensional case to simplify the analysis, knowing that the same analysis applies to the multidimensional case (2 and 3 D). In addition, the elastodynamic wave equation is reduced to the Helmholtz wave equation in the frequency domain, a case for which theoretical aspects are available and validated in the literature.

This study is organized as follows: in section (II), a general description of the problem considered is presented. The variational formulation of the standard FEM, called continuous Galerkin (CG), is developed. A numerical example is presented. Then, in section (III), the variational formulation of the internal penalty discontinuous Galerkin methods is studied. The results of the numerical experiments are shown. A discussion on the obtained algebraic system characteristics is exposed. Finally, a conclusion in section (IV) summarizes the study and its interest to future work.

II. Continuous Galerkin method

In this section, we present the considered problem and the variational formulation of the classical finite element method for spatial discretisation of the second-order wave equation in one dimension. The eigenvalue problem being built, a numerical example is presented.

A. General description of the problem

Consider a bar with an arbitrary cross-section (A) uniform along the propagation axis, of length L and free ends as showed in the figure (1).

Under the assumption of plane deformation and a small cross section relative to the length of the structure, the traction-compression waves in the propagation axis x are

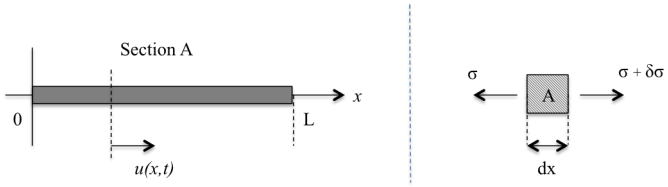

Figure 1. Longitudinal traction-compression waves of a uniform cross-section rod in the axis of propagation x : Axial displacement of an element of the rod.

governed by the second-order wave equation:

$$\frac{\partial^2 u}{\partial t^2} = c_L^2 \frac{\partial^2 u}{\partial x^2}. \tag{1}$$

where $c_L = \sqrt{\frac{E}{\rho}}$ is the speed of propagation of longitudinal waves; ρ is the mass density of the material of the rod; E is Young's modulus; t is the time.

Looking for time-harmonic solutions $u(x,t) = U(x)e^{-i\omega t}$, the equation (1) becomes the reduced Helmholtz wave equation. Taking into account the stress free ends, i.e. null Neumann boundary conditions, the problem is set on the interval $I = [a,b]$ and its limits $\partial I = (a,b)$ such as:

$$\frac{\partial^2 U(x)}{\partial x^2} + k^2 U(x) = 0, \tag{2a}$$

$$\frac{\partial U(x)}{\partial x}|_{\partial I} = 0, \tag{2b}$$

where $k = \dfrac{\omega}{c_L}$ expresses the wave number; ω is the angular frequency.

To analyze the waveguide's behavior, the wave numbers k and the corresponding modes $U(x)$ are to be found. In other words, a Laplace eigenvalue problem is to be resolved. In this simple geometry case, analytical exact solutions are established. There is an infinity of solutions (U^{ex}, k^{ex}), mode shapes and corresponding natural frequencies, such as:

$$\begin{cases} U_m^{ex}(x) = A\,\cos(k_m x), \quad m = 0,1,2,3,... \\ k_m^{ex} = \dfrac{m\pi}{L}. \end{cases} \tag{3}$$

All the solutions k are positive real numbers. The first frequency corresponding to a rigid body motion of the bar is zero ($k = 0$). The second relates to the fundamental mode of the traction-compression of rod, while the rest are its multiples [15].

B. Variational formulation

By means of the method of weighted residuals, multiplying (2a) by a test or a weighting function $v(x)$ and integrating the result on the field I, we get the strong integral form:

$$\int_I \left(\frac{\partial^2 U(x)}{\partial x^2} + k^2 U(x) \right) v(x)\,\mathrm{d}x = 0. \tag{4}$$

Integrating by parts the first term in (4), we obtain the weak form :

$$\begin{aligned}&\left[\frac{\partial U(x)}{\partial x}v(x)\right]_{\partial I}\\&-\int_I \frac{\partial U(x)}{\partial x}\frac{\partial v(x)}{\partial x}\,\mathrm{d}x + k^2\int_I U(x)v(x)\,\mathrm{d}x = 0,\end{aligned} \tag{5}$$

with:

$$\left[\frac{\partial U(x)}{\partial x}v(x)\right]_{\partial I} = \frac{\partial U(b)}{\partial x}v(b) - \frac{\partial U(a)}{\partial x}v(a). \tag{6}$$

The spatial domain is then meshed into a finite number of n identical elements $\{E_j = [x_j, x_{j+1}], j = 0, 1, ..., n-1.\}$ size h. The integral over the whole area is transformed into a sum of integrals over its elements. For an element E_j, we write:

$$\begin{aligned}&\int_{x_j}^{x_{j+1}} \frac{\partial U(x)}{\partial x}\frac{\partial v(x)}{\partial x}\,\mathrm{d}x - k^2\int_{x_j}^{x_{j+1}} U(x)v(x)\,\mathrm{d}x\\&= \frac{\partial U(x_n)}{\partial x}v(x_n) - \frac{\partial U(x_0)}{\partial x}v(x_0),\end{aligned} \tag{7}$$

A change of variables allows to transform the coordinates x_j and x_{j+1} in the coordinate system x into -1 and $+1$ in the local coordinate system of each element ξ. The elementary integrals become:

$$\begin{aligned}\int_{x_j}^{x_{j+1}} \frac{\partial U(x)}{\partial x}\frac{\partial v(x)}{\partial x}\,\mathrm{d}x &= \int_{-1}^{+1} \frac{\partial U}{\partial \xi}\frac{\partial \xi}{\partial x}\frac{\partial v}{\partial \xi}\frac{\partial \xi}{\partial x}\mathrm{det}(J)\,\mathrm{d}\xi,\\ \int_{x_j}^{x_{j+1}} U(x)v(x)\,\mathrm{d}x &= \int_{-1}^{+1} U(\xi)v(\xi)\mathrm{det}(J)\,\mathrm{d}\xi,\end{aligned} \tag{8}$$

where $\det(J)$ is the determinant of the Jacobian matrix such as :

$$\mathrm{det}(J) = \frac{dx}{d\xi} = \frac{\Delta x_j}{2} = \frac{h}{2}, \tag{9}$$

The approximation of the solution function $U(\xi)$ on each element of N nodes is:

$$U^e(\xi) = \sum_{l=0}^{p} P_l(\xi)U_l^e = \mathbf{P}\cdot\mathbf{U}^e, \tag{10}$$

where $\{P_l(\xi), l = 0, 1, ..., p\}$ is the set basis interpolating polynomials of order $p = N - 1$.

Continuous Galerkin method consists of the choice of the test function $v(x)$ equal to the variation of $U(x)$:

$$v(\xi) = \delta U^e(\xi) = \mathbf{P}\cdot\delta\mathbf{U}^e. \tag{11}$$

For simplicity, we use $\delta U^e = (\delta\mathbf{U}^e)^T\mathbf{P}^T$. Substituting the function U by its nodal approximation (10) and the test function $v(x)$ by (11) on the left side of (7), we get:

$$\frac{2}{h}\int_{-1}^{+1}(\delta\mathbf{U}^e)^T\frac{\mathrm{d}\mathbf{P}^T}{\mathrm{d}\xi}\frac{\mathrm{d}\mathbf{P}}{\mathrm{d}\xi}\mathbf{U}^e\,\mathrm{d}\xi - k^2\frac{h}{2}\int_{-1}^{+1}(\delta\mathbf{U}^e)^T\mathbf{P}^T\mathbf{P}\mathbf{U}^e\,\mathrm{d}\xi. \tag{12}$$

Thereby, a system of elementary linear algebraic equations is obtained:

$$(\delta\mathbf{U}^e)^T\left([\mathbf{K}_e] - k^2[\mathbf{M}_e]\right)\mathbf{U}^e, \tag{13}$$

where $[\mathbf{K}_e]$ and $[\mathbf{M}_e]$ are respectively the elementary matrices of mass and stiffness of size $(N\times N)$ such as:

$$\begin{aligned}[\mathbf{K}_e] &= \frac{2}{h}\int_{-1}^{+1}\frac{\mathrm{d}\mathbf{P}^T}{\mathrm{d}\xi}\frac{\mathrm{d}\mathbf{P}}{\mathrm{d}\xi}\,\mathrm{d}\xi,\\ [\mathbf{M}_e] &= \frac{h}{2}\int_{-1}^{+1}\mathbf{P}^T\mathbf{P}\,\mathrm{d}\xi.\end{aligned} \tag{14}$$

The assembly of the latter elementary matrices allows to write:

$$\begin{aligned}&(\delta\mathbf{U})^T\left([\mathbf{K}] - k^2[\mathbf{M}]\right)\mathbf{U}\\&= \frac{\partial U(x_n)}{\partial x}\delta\mathbf{U}(m) - \frac{\partial U(x_0)}{\partial x}\delta\mathbf{U}(1),\end{aligned} \tag{15}$$

where $[\mathbf{K}]$ and $[\mathbf{M}]$ are the global matrices of size $(m\times m)$ with $m = p*n+1$; $\mathbf{U}$ is the global vector of m generalised nodal displacements.

Finally, factoring and simplifying by $\delta\mathbf{U} \neq 0$, the global system is obtained in the following standard form:

$$\left([\mathbf{K}] - k^2[\mathbf{M}]\right)\mathbf{U} = \mathbf{F}, \tag{16}$$

where, in the absence of body forces, $\mathbf{F} = [F_L\ \mathbf{0}\ F_R]^T$ is the global vector of time harmonic forces.

C. Eigenvalue problem

The free harmonic wave propagation (i.e. modal analysis) in a system occurs when external forces and constraints border are zero (2b); F_R and F_L equal zero and so is $\mathbf{F} = 0$. Thus, the algebraic system (16) becomes the generalised eigenproblem (GEP):

$$\left([\mathbf{K}] - \lambda[\mathbf{M}]\right)\mathbf{U} = \mathbf{0}, \tag{17}$$

where $\lambda = k^2$ is a positive real scalar. This system of m linear equations admits m non-trivial solutions (λ_i, U_i) satisfying:

$$\left([\mathbf{K}] - \lambda_i[\mathbf{M}]\right)\mathbf{U}_i = \mathbf{0}, \tag{18}$$

where the quantities $\lambda_i = k_i^2$ $(i = 1, 2, ..., m)$ are the roots of the algebraic equation:

$$\det\left([\mathbf{K}] - \lambda[\mathbf{M}]\right) = \mathbf{0}. \tag{19}$$

Solving (17) provides the traction-compression mode shapes - the eigenfunction $\mathbf{U}_i$ and the corresponding numerical wave numbers $k_i = \sqrt{\lambda_i}$. Note that $\lambda_1 \simeq 0$ and its own mode $U_1(x) = cte$, where cte means constant, corresponds to a rigid body motion.

1) Numerical example: Consider a bar of length $L = 60\ m$ on the interval $I = [-1.59]$. The domain is meshed in 300 linear Lagrange elements. Figure (2) shows the first 6 solutions $\{(\mathbf{U}_i, k_i), i = 1, 2, .., 6\}$. The amplitudes of the eigenmodes of each curve are normalized with respect to their respective maximums.

III. Discontinuous Galerkin methods

In this section, the derivation of the class of discontinuous methods known as interior penalty family is presented. Then, the algebraic system being constructed and the boundary conditions applied, the eigenvalue problem is solved. The discontinuous system features are discussed.

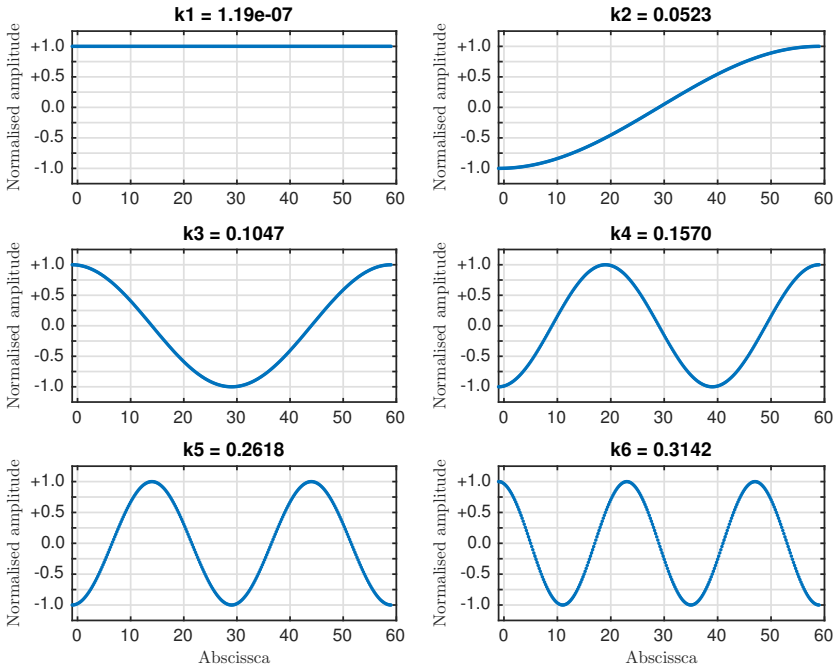

Figure 2. The first 6 eigenmodes of traction-compression and the corresponding numerical wave numbers.

A. *Discontinuous variational formulation*

Unlike the continuous Galerkin formulation which consists of integrating over the whole domain, the discontinuous formulation is locale. The solution is sought in each element separately. So the starting point is essentially different.

Consider the problem defined in (2a). As shown in Figure (3), the spatial domain $I = [a, b]$ is meshed into a finite number of n elements $E_j = [x_j, x_{j+1}]$ where $j = 0, .., n-1$ is the index of the element.

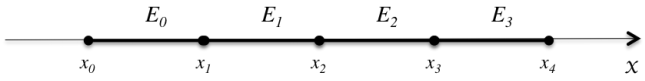

Figure 3. Mesh of the domain I.

We define the size of the element by:

$$h_j = x_{j+1} - x_j, \qquad h_{max}(j) = max(h_{j-1}, h_j).$$

The essential idea of the method is derived from the fact that the weighting functions can be chosen so that the field variable, or its derivatives or usually both, are considered discontinuous across the boundaries of the element while the continuity of the domain is maintained. Therefore, we define $\mathcal{D}_p$ the space of the discontinuous piecewise test functions $v(x)$ on the mesh $I_h = \sum_j E_j$:

$$\mathcal{D}_p(I_h) = \{v : v\mid_{E_j} \in \mathbb{P}_p(E_j) \quad \forall j = 0, .., n-1\},$$

where $\mathbb{P}_p(E_j)$ is the space of interpolation polynomials of order p in the element E_j. Therefore, it is wise to note that for $v\mid_{E_j}$ defined only in inside, we write:

$$v(x_j) = v(x_j^+) = \lim_{\substack{\epsilon \to 0 \\ \epsilon > 0}} v(x_j + \epsilon),$$
$$v(x_{j+1}) = v(x_{j+1}^-) = \lim_{\substack{\epsilon \to 0 \\ \epsilon > 0}} v(x_{j+1} - \epsilon),$$

By means of the weighted residuals method, multiplying (2a) by a discontinuous test function $v(x)$ and integrating the result of the element E_j, the elementary strong integral form is obtained:

$$\int_{x_j}^{x_{j+1}} \left(\frac{\partial^2 U(x)}{\partial x^2} + k^2 U^{(j)}(x) \right) v(x)\, \mathrm{d}x = 0, \tag{20}$$

To get the elementary weak integral form, we integrate by parts the first term in (20). We obtain:

$$\begin{aligned} &\int_{x_j}^{x_{j+1}} \frac{\partial U(x)}{\partial x} \frac{\partial v(x)}{\partial x}\, \mathrm{d}x - k^2 \int_{x_j}^{x_{j+1}} U(x) v(x)\, \mathrm{d}x \\ &- \left[\frac{\partial U(x)}{\partial x} v(x) \right]_{x_j}^{x_{j+1}} = 0, \end{aligned} \tag{21}$$

In CG formulation, the approached the displacement field is forced to be continuous across the borders of the elements - a direct consequence of global matrices. In contrast, the DG formulation allows the field to be discontinuous across the borders. Therefore, solutions on the interfaces are duplicated. As illustrated in Figure (4), there is no coupling between the elements and the values are not unique.

For this reason, a treatment of this inter-element discontinuity is necessary to complete the discretisation. Thus, the values at the borders are to be calculated based on the two

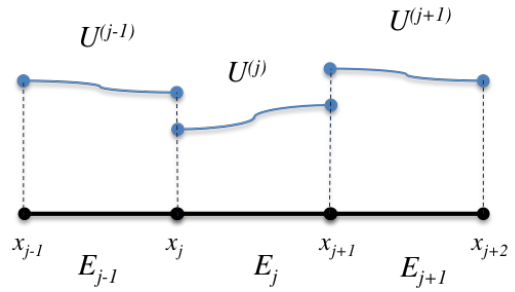

Figure 4. Discontinuity and duplication of values at the inter-elements borders.

values available:

$$\begin{aligned} U(x)|_{\partial E_j} &= f_0(U_L, U_R), \\ \partial U(x)|_{\partial E_j} &= f_1(\partial U_L, \partial U_R), \end{aligned} \tag{22}$$

where ∂/U_L and ∂/U_R are respectively the values of $\partial/U(x)$ on the left and the right of the element interfaces ∂E_j. This treatment is based on the use of a numerical flux as demonstrated by Cockburn et al. [16], which must be carefully defined since it dramatically affects the stability and the accuracy of the method.

In order to establish this numerical flux, it is necessary to define first the jump $[[\bullet]]$ and average $\{\{\bullet\}\}$ across the interface between two adjacent elements:

$$\begin{aligned} [\![\cdot]\!] &= (\cdot\,|_L) - (\cdot\,|_R), \\ \{\{\cdot\}\} &= q_L(\cdot\,|_L) + q_R(\cdot\,|_R), \end{aligned} \tag{23}$$

where q_L and q_R are respectively the coefficients of the average of the element on the left and the right of the interface considered. This definition of the average is general. However, in this work we limit ourselves to the special case where $q_L = q_R = \frac{1}{2}$.

Considering the above definitions, the weak integral form (21) becomes:

$$\begin{aligned} &\int_{x_j}^{x_{j+1}} \frac{\partial U(x)}{\partial x}\frac{\partial v(x)}{\partial x}\,\mathrm{d}x - k^2\int_{x_j}^{x_{j+1}} U(x)v(x)\,\mathrm{d}x \\ &- \left(\{\{\frac{\partial U(x_{j+1})}{\partial x}\}\}v(x_{j+1}^-) - \{\{\frac{\partial U(x_j)}{\partial x}\}\}v(x_j^+)\right) = 0. \end{aligned} \tag{24}$$

By summing for all the elements, we get:

$$\begin{aligned} &\sum_{j=0}^{n-1}\int_{x_j}^{x_{j+1}} \left(\frac{\partial U(x)}{\partial x}\frac{\partial v(x)}{\partial x} - k^2U(x)v(x)\right)\mathrm{d}x \\ &- \sum_{j=0}^{n}\{\{\frac{\partial U(x_j)}{\partial x}\}\}[\![v(x_j)]\!] = 0. \end{aligned} \tag{25}$$

It is important to mention that this formulation remains general and incomplete. The solution is neither convergent nor stable. The existence and the uniqueness of the solution can not be demonstrated. Moreover, it does not include a treatment of the boundary conditions [17]. This will be the subject of the next paragraph.

1) Interior penalty method: To obtain a valid method, the numerical flux allowing information transmission between the different elements must always and imperatively satisfy the conditions of consistency, conservation and cœrcivity [16] [18]. Starting from the first condition, the exact solution U^{ex} must satisfy:

$$\begin{aligned} [\![U^{ex}]\!] &= 0, \\ [\![\frac{\partial U^{ex}}{\partial x}]\!] &= 0. \end{aligned} \tag{26}$$

In this case, under the consistency hypothesis, it is legitimate to add a term which vanishes when the numerical solution is the right approximation of the exact one. In other words, the penalty function:

$$g(U, v, \varepsilon) = \varepsilon\sum_{j=0}^{n}\{\{\frac{\partial v(x_j)}{\partial x}\}\}[\![U(x_j)]\!], \tag{27}$$

where ε is generally a real number to adjust.

By incorporating this function in (25), it yields the basic expression of the interior penalty discontinuous Galerkin formulation:

$$\begin{aligned} &\sum_{j=0}^{n-1}\int_{x_j}^{x_{j+1}} \left(\frac{\partial U(x)}{\partial x}\frac{\partial v(x)}{\partial x} - k^2U(x)v(x)\right)\mathrm{d}x \\ &- \sum_{j=0}^{n}\{\{\frac{\partial U(x_j)}{\partial x}\}\}[\![v(x_j)]\!] + \varepsilon\sum_{j=0}^{n}\{\{\frac{\partial v(x_j)}{\partial x}\}\}[\![U(x_j)]\!] = 0 \end{aligned} \tag{28}$$

Indeed, there are three cases of ε in the literature. In each case, a sub-method can be identified. But before addressing this classification, it should be noted that some of these sub-methods require other types of penalty for them to be coercive [17]. Hence, there are two more types of penalties involving the approximate function and its derivative, respectively:

$$\begin{cases} J_0(U, v, \alpha) = \displaystyle\sum_{j=0}^{n}\frac{\alpha}{h_{max}(j)}[\![U(x_j)]\!][\![v(x_j)]\!], \\ J_1(U, v, \gamma) = \displaystyle\sum_{j=1}^{n-1}\frac{\gamma}{h_{max}(j)}[\![\frac{\partial U(x_j)}{\partial x}]\!][\![\frac{\partial v(x_j)}{\partial x}]\!], \end{cases} \tag{29}$$

where α and γ are two positive real numbers.

At last, by adding these last two functions in (28), we obtain the general expression of the IPDG approximation of the Laplacian operator:

$$\begin{aligned} &\sum_{j=0}^{n-1}\int_{x_j}^{x_{j+1}} \left(\frac{\partial U(x)}{\partial x}\frac{\partial v(x)}{\partial x}\,\mathrm{d}x - k^2U(x)v(x)\,\mathrm{d}x\right) \\ &- \sum_{j=0}^{n}\{\{\frac{\partial U(x_j)}{\partial x}\}\}[\![v(x_j)]\!] + \varepsilon\sum_{j=0}^{n}\{\{\frac{\partial v(x_j)}{\partial x}\}\}[\![U(x_j)]\!] \\ &+ \sum_{j=0}^{n}\frac{\alpha}{h_{max}(j)}[\![U(x_j)]\!][\![v(x_j)]\!] \\ &+ \sum_{j=1}^{n-1}\frac{\gamma}{h_{max}(j)}[\![\frac{\partial U(x_j)}{\partial x}]\!][\![\frac{\partial v(x_j)}{\partial x}]\!] = 0, \end{aligned} \tag{30}$$

The derivations of IPDG method established in the literature corresponding to $\varepsilon = \{-1; 0; +1\}$ are accordingly : the symmetric interior penalty method (SIPDG), incomplete interior penalty method (IIPDG) and non-symmetric penalty interior (NIPDG). Details of their development and implementation are omitted here, however a more general mathematical analysis, implementation aspects and a detailed bibliography can be found in these references [11] [19] [17].

Furthermore, it is important to highlight that there are combinations of ε, α and γ which give unstable methods. For example, in (25) when $\varepsilon = \alpha = \gamma = 0$, the solution is neither convergent nor stable. As for the variants defined above, the existence, the uniqueness and the stability conditions of the solution are shown in [17].

2) Neumann boundary conditions: In the context of discontinuous methods such as the IPDG, the implementation of boundary conditions (BC) is a complicated task. The only information exchanged between neighboring elements is through the numerical flux on the common interface. Therefor, this connection is the key to their implementation. However, the peculiarity of the Neumann BC type (2b) is that they satisfy directly the integral on the borders of the domain ∂I_h. Like this, the corresponding jump and average involving U and ∂U are zero. Thus, the term of this integral can be moved directly to the right hand of (30).

$$\begin{aligned}\int_{\partial I_h} \frac{\partial U(x)}{\partial x} v(x)\,\mathrm{d}x &= \left[\frac{\partial U(x)}{\partial x} v(x)\right]_a^b \\ &= \frac{\partial U(b)}{\partial x} v(x_n^-) - \frac{\partial U(a)}{\partial x} v(x_0^+).\end{aligned} \tag{31}$$

Finally, the DG scheme is complete. The problem can be defined as:

Find $U \in \mathcal{D}_p(I_h)$ such that :

$$\forall v \in \mathcal{D}_p(I_h), \qquad a_\varepsilon(U, v) = \mathcal{L}(v). \tag{32}$$

where the bilinear form $a_\varepsilon(U, v)$ and linear form $\mathcal{L}(v)$ are defined as:

$$\begin{aligned}a_\varepsilon(U,v) = &\sum_{j=0}^{n-1} \int_{x_j}^{x_{j+1}} \left(\frac{\partial U(x)}{\partial x}\frac{\partial v(x)}{\partial x}\,\mathrm{d}x - k^2 U(x)v(x)\,\mathrm{d}x \right) \\ &- \sum_{j=1}^{n-1} \{\{\frac{\partial U(x_j)}{\partial x}\}\}[\![v(x_j)]\!] + \varepsilon \sum_{j=1}^{n-1} \{\{\frac{\partial v(x_j)}{\partial x}\}\}[\![U(x_j)]\!] \\ &+ \sum_{j=1}^{n-1} \frac{\alpha}{h_{max}(j)} [\![U(x_j)]\!][\![v(x_j)]\!] \\ &+ \sum_{j=1}^{n-1} \frac{\gamma}{h_{max}(j)} [\![\frac{\partial U(x_j)}{\partial x}]\!][\![\frac{\partial v(x_j)}{\partial x}]\!], \\ \mathcal{L}(v) = &\frac{\partial U(b)}{\partial x} v(x_n^-) - \frac{\partial U(a)}{\partial x} v(x_0^+).\end{aligned} \tag{33}$$

B. Eigenvalue problem

Likewise, the global linear algebraic system resulting from the discretisation of the weak formulation (33) in conservative free regime ($\{\mathbf{F}\} = 0$) is an eigenvalue problem. It can be rewritten in the following generalized form:

$$\left([\mathbf{A}^{KE}] - \lambda[\mathbf{A}^{M}]\right)\{\mathbf{U}\} = \mathbf{0}, \tag{34}$$

where $\lambda = k^2$ is a positive real scalar; $[\mathbf{A}^{KE}]$ and $[\mathbf{A}^{M}]$ are the global stiffness-flux and mass matrices respectively. They are square matrices of size $(m \times m)$ with $m = n * (p + 1)$, called block or partitioned matrices. The mass matrix is block diagonal, while the stiffness-flux matrix is block tridiagonal; $\{\mathbf{U}\}$ is the global generalized nodal displacement vector.

1) Numerical example: Consider a bar of length $L = 60$. The physical domain is meshed into n Lagrange linear elements ($p = 1$) of the same size h. The IPDG derivations (Symmetric, Non-symmetric and Incomplete) are all used with a factor $\gamma = 0$. The penalty parameter is chosen such that $\alpha = 3/h > 0$, in order to ensure stability.

Figure (5) shows the discontinuous mode shape and the corresponding numerical wave number of the first six modes $\{(\mathbf{U}_i, k_i), i = 1, 2, .., 6\}$ resulting from the IIPDG eigenproblem. Each element is drawn independently from each other in a discontinuous manner with a different color and dots indicating the degree of freedom of the element. Amplitudes are normalized with respect to the global vector $\mathbf{U}_i$ maximum.

The table(1) presents the numerical dispersion error on the wavenumbers as well as the L^2 error norm obtained for the first six modes $\{(\mathbf{U}_i, k_i), i = 1, .., 6\}$ on the mesh I_h. They are, as defined in [20]:

(i) Numerical dispersion error on the wavenumber k_i :

$$\mathcal{E}_k = |k_{ex} - k_{num}|;$$

(ii) L^2 error norm on the mode shape $\mathbf{U}_i$:

$$\|\mathcal{E}_h\|_{L^2} = \sqrt{\sum_{j=0}^{n} (U^{ex}(x_j) - U^{num}(x_j))^2}.$$

Subsequently, the convergence rate, the speed at which the solution converges (i.e. the error decreases) depending on the size of the mesh h, is calculated for the eigenmodes and their corresponding wavenumbers resulting from each sub-method GEP. In fact, the error can be written as:

$$\mathcal{E}(h) = Ch^\beta,$$

where

$$\beta = \frac{1}{\ln(2)} \ln\left(\frac{\mathcal{E}|_h}{\mathcal{E}|_{h/2}}\right).$$

is said the order of accuracy (id. convergence rate) of the method in space.

Table (2) shows these rates for the eigenvalues and the eigenfunctions in the L^2 norm obtained from the three sub-methods for $n = 150$ and $n * 2 = 300$ corresponding to $h = 0.4$ and $h/2 = 0.2$.

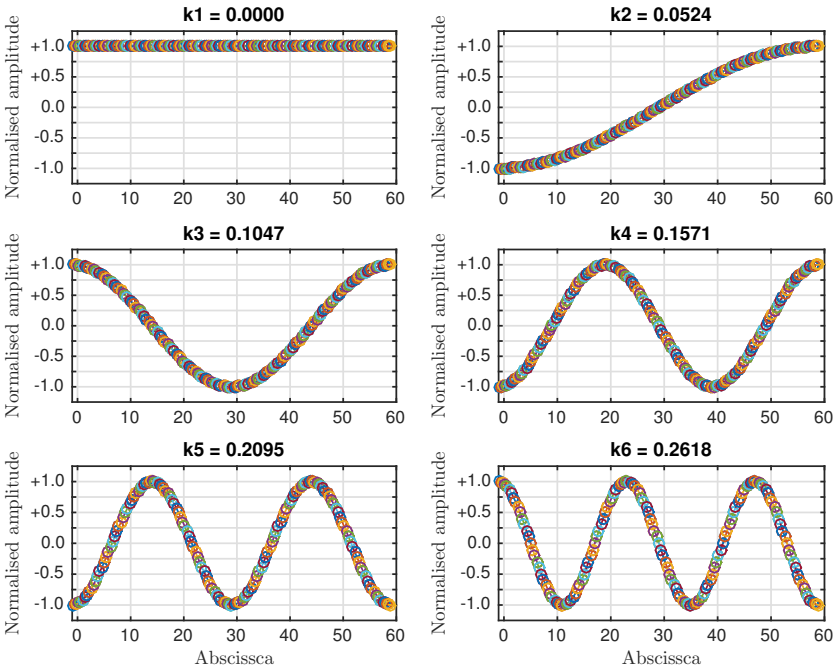

Figure 5. The first 6 eigenmodes and wavenumbers obtained from resolving the GEP resulting from the IIPDG derivation with $\alpha = 3/h$ and $\gamma = 0$.

Table I. THE NUMERICAL DISPERSION ERROR AND L^2 ERROR NORM FOR THE FIRST 6 SOLUTIONS $(\mathbf{U}_i, k_i)$ OBTAINED FROM THE RESOLUTION OF GEP USING $n = 150$ ELEMENTS.

SIPDG

mode i	1	2	3
	4	5	6
$\mathcal{E}_k$	$8.3780e^{-8}$	$9.5692e^{-7}$	$7.6538e^{-6}$
	$2.5823e^{-5}$	$6.1181e^{-5}$	$1.1942e^{-4}$
$\|\mathcal{E}_h\|_{L^2}$	$1.3236e^{-11}$	$4.6879e^{-6}$	$3.7495e^{-5}$
	$1.2650e^{-4}$	$2.9970e^{-4}$	$5.8496e^{-4}$

IIPDG

mode i	1	2	3
	4	5	6
$\mathcal{E}_k$	$8.3780e^{-8}$	$3.1899e^{-7}$	$2.5519e^{-6}$
	$8.6122e^{-6}$	$2.0413e^{-5}$	$3.9866e^{-5}$
$\|\mathcal{E}_h\|_{L^2}$	$1.6168e^{-11}$	$3.1253e^{-6}$	$2.4999e^{-5}$
	$8.4351e^{-5}$	$1.9988e^{-4}$	$3.9021e^{-4}$

NIPDG

mode i	1	2	3
	4	5	6
$\mathcal{E}_k$	$5.7876e^{-8}$	$1.4049e^{-11}$	$4.4776e^{-10}$
	$3.400e^{-9}$	$1.4328e^{-8}$	$4.3724e^{-8}$
$\|\mathcal{E}_h\|_{L^2}$	$1.5060e^{-11}$	$2.3440e^{-6}$	$1.8750e^{-5}$
	$6.3270e^{-5}$	$1.4994e^{-4}$	$2.9275e^{-4}$

Table II. CONVERGENCE RATES OF THE IPDG METHODS FOR THE FIRST 6 SOLUTIONS $(\mathbf{U}_i, k_i)$ IN A UNIFORM MESH WITH $h = 0.4$ AND $h/2 = 0.2$.

SIPDG

mode i	1	2	3	
	4	5	6	
$\beta(k)$	0.3779	1.9999	1.9997	-
	1.9993	1.9988	1.9982	$\simeq 2$
$\beta(U)$	2.6635	2.4999	2.4997	$\simeq 2.5$
	2.4993	2.4987	2.4980	

IIPDG

mode i	1	2	3	
	4	5	6	
$\beta(k)$	0.0894	2.0000	2.0000	-
	1.9999	1.9999	1.9998	$\simeq 2$
$\beta(U)$	6.4006	2.4999	2.4998	$\simeq 2.5$
	2.4995	2.4992	2.4987	

NIPDG

mode i	1	2	3	
	4	5	6	
$\beta(k)$	1.6543	4.7580	4.0055	-
	4.0010	4.0000	3.9999	$\simeq 4$
$\beta(U)$	3.9869	2.5000	2.4998	$\simeq 2.5$
	2.4996	2.4994	2.4990	

First, the obtained results shown in Figure (5) and in Table (1) are in good agreement with those obtained in the numerical example of the continuous formulation in section (II). Second, in agreement with the results found in literature in [12] [13], the solutions provided by all the IPDG derivations are spectrally correct, as well as the multiplicity. They are free of spurious modes as the stability condition $\alpha > 0$ is widely verified. The modal base, the spectrum and the eigenmodes space, is complete.

Furthermore, from the results of Table (2): the symmetric and non-symmetric methods provide a second-order precision approximation in the dispersion error on the wavenumber, while the incomplete derivative provides an approximation of fourth order of accuracy. Moreover, the rate of convergence in the L^2 error norm of the eigenfunctions is the same for the whole IPDG family. Finally, we note that these latter results depend on the penalty value α and the polynomial order.

2) Advantages and disadvantages of the discontinuous system: The local nature of the DG formulation leads to a duplication of the freedom degrees on the neighboring elements borders. This, in the context of the temporal evolution and initial value problems constitutes the major drawback of the method since it increases the computational cost for a same solution U.

However, in the context of eigenvalue problem this attribute is double-edged since the unknown here is the couple $(\lambda_i, \mathbf{U}_i)$. On the one hand, to the natural modes $\mathbf{U}_i$ it's still a heavy disadvantage. Nevertheless, it can be reduced by decreasing the number of border nodes and introducing internal nodes. This is done by increasing the degree of the polynomials basis of the numerical solution (i.e. *p*-refinement-).

On the other hand, this duplication has an interesting effect on the eigenvalues λ_i. In a point x_j, two solutions are computed on the left and the right respectively $U_i(x_j^-)$ and $U_i(x_j^+)$. These latter when the solution $\mathbf{U}_i$ tends to the exact one, become two sides of the same coin: $U_i(x_j^-) = U_i(x_j^+)$. Meanwhile, calculated eigenvalues corresponding to these two points are still distinct.

In fact, a problem (34) of order m provides m solutions λ_i. In the CG formulation , the problem is of size $\{(m\times m),\ m = (n*p)+1\}$, whereas in the DG solution it is of size $\{(m\times m),\ m = n*(p+1)\}$. Ergo, for the same order m, thus a same number of solutions k_i we have:

$$\begin{cases} m_{CG} = m_{DG}, \\ m_{DG} = n_{DG} * (p_{DG}+1), \end{cases} \tag{35}$$

with

$$n_{DG} = \frac{(n_{CG} * p_{CG}) + 1}{p_{DG}+1}. \tag{36}$$

This means that in the context of high order methods, the n_{DG} is always less than n_{CG}. For example, for $p_{DG} = p_{CG} = 1$, the number of elements n_{DG} is equal to about half the number of elements required in CG formulation. Thus, the solutions λ_i are obtained with fewer elements than the CG, so less time consumed in calculating elementary matrices and assembly.
Consequently, for wave numbers oriented computations like dispersion curves calculations, the DG methods are suitable since the same solution curves can be obtained with less elements.

In addition, the mass matrix is block-diagonal. Hence, its inverse is the block diagonal matrix of the inverse of the blocks separately:

$$[\mathbf{M}^{-1}] = \begin{pmatrix} [\mathbf{M}_0^{-1}] & 0 & \cdots & 0 \\ 0 & [\mathbf{M}_1^{-1}] & \cdots & 0 \\ \vdots & \vdots & \ddots & \vdots \\ 0 & 0 & \cdots & [\mathbf{M}_{n-1}^{-1}] \end{pmatrix} \tag{37}$$

These inverse elementary matrices can be calculated independently and multiplied directly to build the dynamic stiffness matrix $[\mathbf{A}_g] = [\mathbf{M}^{-1}\mathbf{K}]$. Therefore, the assembly of the mass matrix is unnecessary, an operation that is well known to be too expensive in computation time. Besides, the matrix $[\mathbf{A}_g]$ keeps its block-tridiagonal shape. Thus, the GEP is reduced into a standard problem. This transformation for large problems can lead to a significant gain in computation time.
The standard form problem is given by:

$$([\mathbf{A}_g] - \lambda[\mathbf{I}])\{\mathbf{U}\} = \mathbf{0}, \tag{38}$$

where $[\mathbf{I}]$ is the identity matrix of order m.

Aside from that, it is well known that the extraction of the eigenvalues is the most costly problem in terms of calculation even for a standard problem. Nonetheless, the discontinuous system (40) is even more interesting thanks to its block-tridiagonal form for which numerous competitive modal extraction methods based on the Divide-and-Conquer computational techniques are developed in the literature. This new generation of effective and suitable for parallel execution algorithms operates on multiple portions/blocks at the same time instead of scalars. They use decomposition and multiplication block-algorithms such as LU, QR, Cholskey, Strassen, etc. Therefore, they require fewer operations and less storage especially for a block-tridiagonal matrices and even less for symmetric positive definite ones (for more details see [21] [22] [23] [24]). Therewith, their gain increases with the size of the blocks, which is perfectly in line with the desired solution. By increasing the size of local matrices, i.e. the polynomial order p, the number of blocks in the global matrix is reduced and so is the number of operations. In this way, the computational time and the accuracy are optimised.

IV. Conclusions and future work

In this work, a modal analysis of a free end finite 1-D structure is performed in order to study the potential benefits of the discontinuous Galerkin methods when applied to harmonic wave propagation eigenvalue problems; this is in the aim for a subsequent application in the ultrasonic guided waves SHM area. In this sens, the second-order wave equation in one dimension of space is discretised using both continuous and discontinuous Galerkin methods; the corresponding problems were constructed; numerical examples were shown; and finally the advantages and disadvantages of the discontinuous system over the continuous one were discussed.

First, a good agreement between the results of the two formulations is observed. In agreement with works in the literature, the approximations obtained are spectrally correct and free of spurious modes for all the interior penalty discontinuous Galerkin methods family: symmetric, non-symmetric and incomplete.

In addition, the results confirmed an optimal convergence of the wave number for non-symmetric derivation (of precision order $\beta = 4$), while for the symmetric and incomplete methods, a convergence of the second order is obtained; which is typical of the continuous method. Further on, the rate of convergence in the L^2 norm of the eigenfunctions is the same for the whole IPDG family.
Indeed, these results depend on the penalty value α and the selected polynomial order. The question on the influence and role of the penalty as a function of the polynomial

order is still to be detailed in a future work in the context of analysis and comparison of performances of IPDG methods.

Moreover, unlike the development of DG methods in the time domain ensuring naturally parallelisable numerical schemes and unnecessary matrices assembly, for eigenproblems the method requires at least an assembly operation and a global system resolution. The elementary solution can not be obtained directly and independently of the global solution, withal the multiplicity and complicity of the sought solutions in such problems. However, all calculations done, the discontinuous method is advantageous compared to the continuous one, particularly in the oriented wavenumbers calculations like dispersion curves which is consistent with our future work for an application in the field of structural health monitoring.

The discontinuous system is still attractive because of its natural block partitioned form that allows to convert the problem from generalised to standard form while saving an assembly operation. Likewise, it enables the use of very fast, efficient and highly parallel block-algorithms. Besides, the performance of the resulting solvers is scalable according to the increasing size of elementary blocks, so the polynomial order. Therefore, in the context of high-order methods, the DG formulation allows a double gain strategy: less computational time/memory consumption and a high-order achieved accuracy.

REFERENCES

[1] F. Benmeddour, "Étude expérimentale et numérique de l'interaction des ondes de Lamb en présence d'endommagements dans des structures d'aluminium," Thèse doctorat, Université de Valenciennes et du Hainaut-Cambrésis, France, 2006.

[2] B. A. Auld, *Acoustic fields and waves in solids*, 2nd ed. , vol. 2. R.E. Krieger publishing company, Malabar, Florida, 1973.

[3] J. J. Ditri, "Utilization of guided elastic waves for the characterization of circumferential cracks in hollow cylinders," *The Journal of the Acoustical Society of America*, vol. 96, no. 6, p. 3769, 1994.

[4] T. Hayashi, W.-J. Song, and J. L. Rose, "Guided wave dispersion curves for a bar with an arbitrary cross-section, a rod and rail example," *Ultrasonics*, vol. 41, no. 3, pp. 175–183, May 2003.

[5] T. Hayashi, C. Tamayama, and M. Murase, "Wave structure analysis of guided waves in a bar with an arbitrary cross-section," *Ultrasonics*, vol. 44, no. 1, pp. 17–24, Jan. 2006.

[6] F. Benmeddour, F. Treyssède, and L. Laguerre, "Numerical modeling of guided wave interaction with non-axisymmetric cracks in elastic cylinders," *International Journal of Solids and Structures*, vol. 48, no. 5, pp. 764–774, Mar. 2011.

[7] P. W. Loveday, "Guided Wave Inspection and Monitoring of Railway Track," *Journal of Nondestructive Evaluation*, vol. 31, no. 4, pp. 303–309, 2012.

[8] W. H. Reed and T. R. Hill, "Triangular Mesh Methods for the Neutron Transport Equation," Los Alamos Scientific Lab., N.Mex. (USA), Tech. Rep. LA-UR–73-479; CONF-730414–2, Oct. 1973.

[9] B. Cockburn, G. E. Karniadakis, C.-W. Shu, M. Griebel, D. E. Keyes, R. M. Nieminen, D. Roose, and T. Schlick, Eds., *Discontinuous Galerkin Methods*, ser. Lecture Notes in Computational Science and Engineering. Berlin, Heidelberg: Springer Berlin Heidelberg, 2000, vol. 11.

[10] B. Cockburn, "Discontinuous Galerkin methods," *ZAMM*, vol. 83, no. 11, pp. 731–754, Nov. 2003.

[11] D. N. Arnold, F. Brezzi, B. Cockburn, and L. D. Marini, "Unified analysis of discontinuous Galerkin methods for elliptic problems," *SIAM journal on numerical analysis*, vol. 39, no. 5, pp. 1749–1779, 2002.

[12] J. S. Hesthaven and T. Warburton, "High-order nodal discontinuous Galerkin methods for the Maxwell eigenvalue problem," *Philosophical Transactions of the Royal Society A: Mathematical, Physical and Engineering Sciences*, vol. 362, no. 1816, pp. 493–524, Mar. 2004.

[13] P. F. Antonietti, A. Buffa, and I. Perugia, "Discontinuous Galerkin approximation of the Laplace eigenproblem," *Computer Methods in Applied Mechanics and Engineering*, vol. 195, no. 25-28, pp. 3483–3503, May 2006.

[14] J. S. Hesthaven and T. Warburton, *Nodal discontinuous Galerkin methods: algorithms, analysis, and applications*, ser. Texts in applied mathematics. New York, NY: Springer, 2008.

[15] T. Gmür, *Dynamique des structures*. Lausanne: Presses polytechniques et universitaires romandes, 2008.

[16] B. Cockburn, G. Kanschat, and D. Schötzau, "The local discontinuous Galerkin method for linearized incompressible fluid flow: a review," *Computers & Fluids*, vol. 34, no. 4-5, pp. 491–506, May 2005.

[17] B. M. Rivière, *Discontinuous Galerkin methods for solving elliptic and parabolic equations: theory and implementation*, ser. Frontiers in applied mathematics. Philadelphia, Pa: SIAM, Society for Industrial and Applied Mathematics, 2008.

[18] F. Brezzi, B. Cockburn, L. Marini, and E. Süli, "Stabilization mechanisms in discontinuous Galerkin finite element methods," *Computer Methods in Applied Mechanics and Engineering*, vol. 195, no. 25-28, pp. 3293–3310, May 2006.

[19] R. Hartmann, "Numerical Analysis of Higher Order Discontinuous Galerkin Finite Element Methods," Oct. 2008.

[20] R. J. LeVeque, *Finite difference methods for differential equations*, 2006.

[21] R. Schreiber, "Block Algorithms for Parallel Machines," in *Numerical Algorithms for Modern Parallel Computer Architectures*, ser. The IMA Volumes in Mathematics and Its Applications, M. Schultz, Ed. Springer US, 1988, no. 13, pp. 197–207.

[22] N. J. Higham, "Block LU Factorization," in *Accuracy and Stability of Numerical Algorithms*, ser. Other Titles in Applied Mathematics. Society for Industrial and Applied Mathematics, Jan. 2002, pp. 245–258.

[23] F. Magoulès and F.-X. Roux, *Calcul scientifique parallèle cours, exemples avec OpenMP et MPI, exercices corrigés*. Paris: Dunod, 2013.

[24] "LAPACK Users' Guide Third Edition : Block algorithms and their derivation." [Online]. Available: http://www.netlib.org/lapack/lug/